Civil Engineering Infrastructures Journal, 47(1): 89 – 109, June 2014
ISSN: 2322 – 2093

Bearing Capacity of Strip Footings near Slopes Using Lower Bound Limit Analysis

Mofidi, J.[1], Farzaneh, O.[2] and Askari, F.[3*]

[1] M.Sc. of Geotechnical Engineering, School of Civil Engineering, College of Engineering, University of Tehran, P.O.Box: 11155-4563, Tehran, Iran.
[2] Assistant Professor, School of Civil Engineering, College of Engineering, University of Tehran, P.O.Box: 11155-4563, Tehran, Iran.
[3] Assistant Professor, International Institute of Earthquake Engineering and Seismology, Tehran, Iran.

Received: 14 Oct. 2012; Revised: 13 Feb. 2013; Accepted: 03 May 2013

ABSTRACT: Stability of foundations near slopes is one of the important and complicated problems in geotechnical engineering, which has been investigated by various methods such as limit equilibrium, limit analysis, slip-line, finite element and discrete element. The complexity of this problem is resulted from the combination of two probable failures: foundation failure and overall slope failure. The current paper describes a lower bound solution for estimation of bearing capacity of strip footings near slopes. The solution is based on the finite element formulation and linear programming technique, which lead to a collapse load throughout a statically admissible stress field. Three-nodded triangular stress elements are used for meshing the domain of the problem, and stress discontinuities occur at common edges of adjacent elements. The Mohr-Coulomb yield function and an associated flow rule are adopted for the soil behavior. In this paper, the average limit pressure of strip footings, which are adjacent to slopes, is considered as a function of dimensionless parameters affecting the stability of the footing-on-slope system. These parameters, particularly the friction angle of the soil, are investigated separately and relevant charts are presented consequently. The results are compared to some other solutions that are available in the literature in order to verify the suitability of the methodology used in this research.

Keywords: Finite Element Method, Limit Analysis, Lower Bound, Slope, Strip Footing.

INTRODUCTION

Some structures are often forced to be built on or near slopes in civil engineering practices. Such structures mainly include buildings and towers built near slopes, particularly in mountainous countries (e.g. Japan), abutments of bridges, electrical transmission towers, and also buildings that are constructed on or near vertical cuts in urban areas.

Stability of foundations adjacent to slopes is a challenging problem in geotechnical engineering because both overall slope stability and foundation bearing capacity should be taken into consideration.

* Corresponding author E-mail: askari@iiees.ac.ir

Numerous researchers have studied this problem via various methods and solutions, including limit equilibrium techniques (Meyerhof, 1957; Azzouz and Baligh, 1983; Narita and Yamaguchi, 1990; Castelli and Motta, 2008), slip-line methods (Sokolovski, 1960), yield design theory (de Buhan and Garnier, 1994, 1998), finite element method (Georgiadis, 2010), upper bound technique (Davis and Booker, 1973; Kusakabe et al., 1981; Michalowski, 1989; Farzaneh et al., 2008; Shiau et al., 2011) and lower bound technique (Lysmer, 1970; Davis and Booker 1973; Shiau et al., 2011). Georgiadis (2010) and Shiau et al. (2011) studied the problem of footing-on-slope only for undrained loading. In this paper, drained condition is considered and the effect of soil friction angle is investigated. In addition, design charts are presented for both purely cohesive and cohesive-frictional soils.

The limit equilibrium technique is often favored due to its simplicity and applicability in problems with complicated geometry, loading, soil properties and boundary conditions. However, this solution is not as accurate as other solutions such as the slip-line method and bounds theorems of limit analysis. The slip-line method is mathematically robust and accurate but is difficult to use in problems with complex loading conditions or geometries.

Bounds theorems of limit analysis (i.e. upper and lower bounds) are the direct approaches of classical plasticity theory for calculation of collapse load in stability problems. The static and kinematic approaches of limit analysis lead to lower and upper estimation of true collapse load, respectively. As the lower bound solution gives a load that is below the exact ultimate load, it is at safe side and therefore more appealing. During last two decades, numerous researches have been undertaken to simplify the application of bounds theorems (particularly the lower bound theory) in geotechnical engineering problems. The main achievement of these researches was a finite-element limit analysis approach, which allows large and complicated problems to be solved using appropriate computers.

Sloan (1988, 1989), Sloan and Kleeman (1995), Lyamin and Sloan (2002a,b) and Krabbenhoft et al. (2005) developed some efficient finite element formulations for numerical solution of stability problems by limit analysis method. In the current study, the formulation of Sloan (1988) is used. The theory and formulation of the finite-element lower bound method is briefly presented here, and more details can be found in relevant references. In this research, a MATLAB code is also developed for computing the lower bound estimation of bearing capacity of strip footings near slopes.

PROBLEM DEFINITION

The ultimate bearing capacity of a shallow strip footing resting on level homogenous ground can be classically calculated using Terzaghi's equation:

$$p_u = cN_c + qN_q + \frac{1}{2}\gamma N_\gamma B \qquad (1)$$

where N_c, N_q and N_γ are the dimensionless bearing capacity factors, c is the soil cohesion, q is the surcharge, γ is the unit weight of the soil and B is the footing width. Bearing capacity factors depend on internal friction angle of the soil, and can be obtained separately by appropriate assumptions and using the superposition principle. For example, N_c can be determined in weightless soil which has no surcharge ($q, \gamma = 0$) or N_q can be determined in weightless cohesionless soil ($c, \gamma = 0$). The superposition

principle is then applied for calculation of the ultimate bearing capacity using Terzaghi's equation.

The problem of bearing capacity of strip footings adjacent to a slope is shown in Figure 1. Geometric parameters include the slope angle β, distance of footing from the slope a, footing width B and height of the slope H. It is assumed that the soil obeys the associated flow rule and Mohr-Coulomb yield criterion, and has the cohesion of c, internal friction angle of ϕ and unit weight of γ. The footing is assumed to be smooth and rigid.

Complexity of a footing-on-slope problem is due to the combination of two interactive problems: the overall stability of the slope and the bearing capacity of the footing itself. Unlike the problem of a strip footing resting on level ground, the limit behavior of a footing-on-slope system is notably influenced by the weight of the soil mass. So, the assumption of a weightless soil is not reasonable in this case and the bearing capacity factors are not calculated separately. Herein, the limit pressure gained from the lower bound theory is presented as the ultimate bearing capacity of the footing-on-slope system. The approach followed in this paper is to consider the normalized limit pressure as a function of dimensionless parameters affecting the stability of the so-called system, which can be stated as:

$$\frac{p}{\gamma B} = f(\beta, \frac{a}{B}, \frac{H}{B}, \frac{c}{\gamma B}, \phi) \qquad (2)$$

where p is the average limit pressure under the footing base. All of the above parameters will be discussed separately in the following sections and related design charts will be presented accordingly.

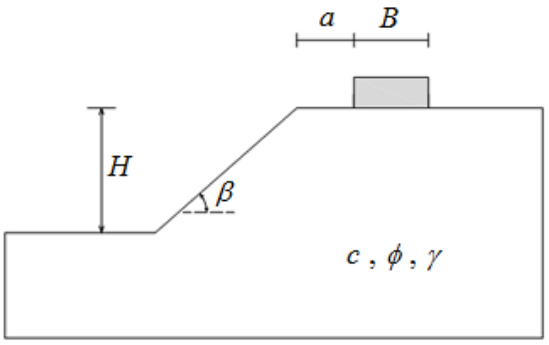

Fig. 1. Problem parameters.

Lower Bound Analysis

The lower bound limit theory (Drucker et al., 1952) can be stated as:

"If all changes in geometry occurring during collapse are neglected, a load obtained from a statically admissible stress field is less than or equal to the exact collapse load."

A statically admissible stress field is one which satisfies equilibrium, the boundary conditions and nowhere violates the yield criterion. The aim of lower bound theory is to maximize the integral below which is called the objective function in the mathematical terminology:

$$P = \int_{A_p} p dA \qquad (3)$$

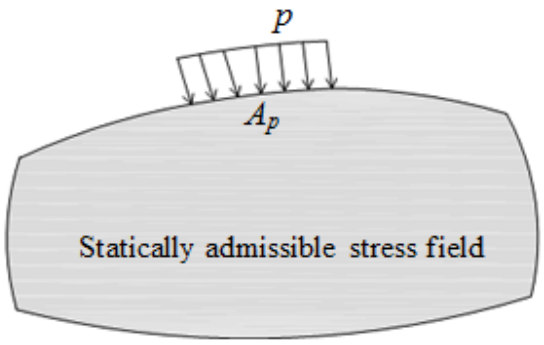

Fig. 2. Lower bound limit pressure.

in which p is the unknown traction acting on the surface area A_p which is to be optimized.

By assembling all equalities and inequalities, the discrete formulation of the lower bound theory leads to following constrained optimization problem: maximize $P(\mathbf{x})$, subject to $\begin{cases} f_i(\mathbf{x}) = 0 \ , \quad i \in I = \{1,\ldots,m\} \\ g_i(\mathbf{x}) \le 0 \ , \quad j \in J = \{1,\ldots,n\} \end{cases}$, where P is the collapse load, $\mathbf{x}$ is the vector of problem unknowns, f_i are the equality functions derived from element equilibrium, discontinuity equilibrium and boundary conditions, while g_j are inequality functions derived from yield criterion and other inequality constraints.

The formulation used in this paper follows that of Sloan (1988) in which the linear finite element method is applied and the domain of the problem is discretized by 3-noded triangular elements. Unknowns of the problem are nodal stresses (σ_x, σ_y, τ_{xy}). Figure 3 shows typical elements and extension elements used in the lower bound limit analysis. The main difference between lower bound mesh and usual finite element mesh is that some nodes may have the same co-ordinate. Thus, the statically admissible stress discontinuities can occur at shared edges of adjacent elements (Figure 4). By using the linear finite elements and linearized yield function, the lower estimation of true collapse load can be obtained through linear programming techniques.

As Lyamin and Sloan (2002a) discussed elaborately, the application of linear finite elements is the most appropriate way for discretizing the domain of the problem in the lower bound theory.

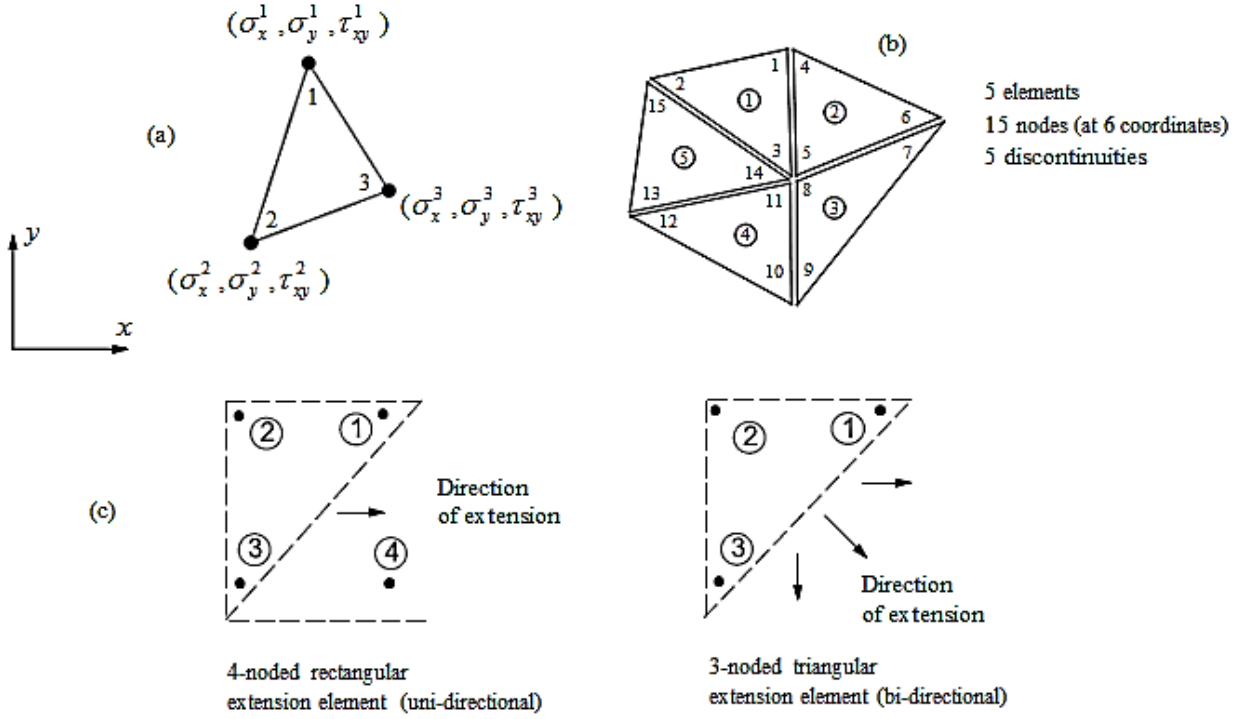

Fig. 3. Typical linear triangular element (a), mesh (b) and extension elements (c) used in lower bound analysis.

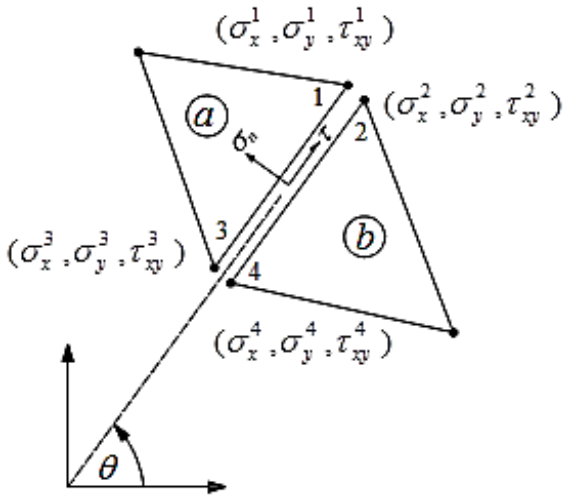

$$\sigma_n = \sin^2\theta\,\sigma_x + \cos^2\theta\,\sigma_y - \sin 2\theta\,\tau_{xy}$$

$$\tau = -\frac{1}{2}\sin 2\theta\,\sigma_x + \frac{1}{2}\sin 2\theta\,\sigma_y + \cos 2\theta\,\tau_{xy}$$

$$\sigma_n^{1a} = \sigma_n^{2b}\ ; \quad \tau^1 = \tau^2$$

$$\sigma_n^{3a} = \sigma_n^{4b}\ ; \quad \tau^3 = \tau^4$$

Fig. 4. Statically admissible stress discontinuity (Shiau et al., 2003).

Thus, the stresses vary linearly throughout an element according to:

$$\sigma_x = \sum_{l=1}^{3} N_l\,\sigma_x^l\ ; \quad \sigma_y = \sum_{l=1}^{3} N_l\,\sigma_y^l\ ; \quad \tau_{xy} = \sum_{l=1}^{3} N_l\,\tau_{xy}^l \tag{4}$$

where σ_x^l, σ_y^l and τ_{xy}^l are nodal stress components and N_l are linear shape functions.

When there is no body force in the x direction and the gravitational force is the only body force in the y direction, equilibrium equations in 2D can be expressed as:

$$\frac{\partial\sigma_x}{\partial x} + \frac{\partial\tau_{xy}}{\partial y} = 0$$
$$\frac{\partial\sigma_y}{\partial y} + \frac{\partial\tau_{xy}}{\partial x} = \gamma \tag{5}$$

Combination of Eqs. (4) and (5) leads to a matrix form of element equilibrium equations.

The Mohr-Coulomb yield criterion in the plain strain condition is stated as:

$$F = (\sigma_x - \sigma_y)^2 + (2\tau_{xy})^2 - (2c.\cos\varphi - (\sigma_x + \sigma_y)\sin\varphi)^2 \le 0 \tag{6}$$

in which tensile stresses are taken as positive. The inequality (6) includes the inner points of a circle in the *X*-*Y* coordinate system with the center of (0, 0) and can be expressed as:

$X^2 + Y^2 \le R^2$

where $X = \sigma_x - \sigma_y$, $Y = 2\tau_{xy}$ and $R = 2c.\cos\varphi - (\sigma_x + \sigma_y)\sin\varphi$. The Mohr-Coulomb yield function is approximated by an interior polygon in the lower bound limit analysis. Figure 5 shows a linearized Mohr-Coulomb yield criterion with m sides and m vertices.

To obtain a rigorous lower bound solution, extension elements (see Figure 3) are used to extend the statically admissible stress field into a semi-infinite domain. The comprehensive details of these types of elements can be found in relevant references (Lyamin, 1999 and Lyamin and Sloan, 2003). Inhere; the special yield conditions of these elements are only presented. Referring to Figure 3, the yield criteria for two types of extension elements are stated as below:

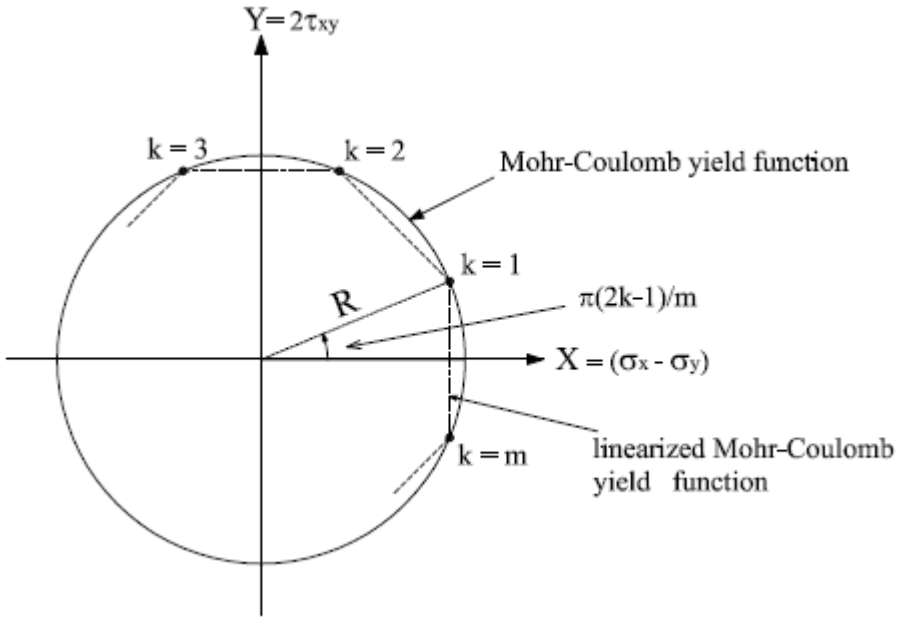

Fig. 5. Linearized Mohr-Coulomb yield function.

$$\begin{cases} f(\boldsymbol{\sigma}^1 - \boldsymbol{\sigma}^2) \le 0 \\ f(\boldsymbol{\sigma}^2) \le 0 \quad : \text{uni} - \text{directional extension element} \\ f(\boldsymbol{\sigma}^3) \le 0 \end{cases} \tag{7}$$

$$\begin{cases} f(\boldsymbol{\sigma}^1 - \boldsymbol{\sigma}^2) \le 0 \\ f(\boldsymbol{\sigma}^2) \le 0 \quad : \text{bi} - \text{directional extension element} \\ f(\boldsymbol{\sigma}^3 - \boldsymbol{\sigma}^2) \le 0 \end{cases} \tag{8}$$

where $\boldsymbol{\sigma}^1, \boldsymbol{\sigma}^2, \boldsymbol{\sigma}^3$ are nodal stress vectors.

Considering equalities and inequalities altogether, the discrete form of the lower bound theory can be expressed as:

$$\begin{aligned} &\text{Maximize } \mathbf{c}^{\mathrm{T}}\boldsymbol{\sigma} \\ &\text{Subject to } \quad \mathbf{A}_1\boldsymbol{\sigma} = \mathbf{b}_1 \\ &\qquad\qquad\quad \mathbf{A}_2\boldsymbol{\sigma} \le \mathbf{b}_2 \end{aligned} \tag{9}$$

where $\mathbf{c}$ is the vector of objective function coefficients, $\mathbf{A}_1$ is the overall matrix of equality constraints which is derived from elements equilibrium, discontinuities equilibrium and boundary conditions, $\mathbf{b}_1$ is the corresponding right-hand vector of equality equations, $\mathbf{A}_2$ is the overall matrix of inequality constraints which is derived from the yield criterion, $\mathbf{b}_2$ is the corresponding right-hand vector of inequality constraints and $\boldsymbol{\sigma}$ is the total vector of unknown stresses.

Since all constraints are linear, Eq. (8) is known as a "linear programming" problem in the mathematical terminology which can be solved by various methods. In this paper, the "active-set" algorithm of the linear programming technique is adopted for solving (optimizing) the finite element form of lower bound analysis. In comparative analyses conducted by the authors, the "active-set" algorithm was more efficient and faster than other algorithms of the linear programming technique such as "simplex" and "interior-point" methods.

Details of Analyses

Based on the finite element formulation of the lower bound method, the bearing capacity of strip footings near slopes is calculated and relevant charts are presented. The current study investigates a range of

dimensionless parameters affecting the stability of the footing-on-slope system, including the slope angle (β), footing distance to the crest of the slope (a/B), height of the slope (H/B), strength ratio due to cohesion ($c/\gamma B$) and internal friction angle of the soil (ϕ). As discussed by Shiau et al. (2011), the footing roughness increases the bearing capacity slightly and the assumption of the smooth footing is conservative in the design of foundations near slopes. So, in the present study, the footing is assumed smooth. The number of sides in the linearized Mohr-Coulomb yield function is assumed 24 in all analyses (i.e. m=24). The domain of the problem is adopted large enough to cover the plastic zone without the presence of the extension elements. Then, in order to obtain a rigorous lower estimation of the true collapse load, the extension elements are used to expand the statically admissible stress field into a semi-infinite domain. To obtain more accurate results, fine meshes are used and stress discontinuities are set between all shared edges of adjacent elements. A typical finite-element mesh for a slope with β =30˚ and (a/B) = 2, consisting of 2168 elements, 6504 nodes and 3199 stress discontinuities, is illustrated in Figure 6. The important note in the stability of footings near slopes is the failure mode of the system, which can be divided into two main modes: the bearing capacity failure and overall slope failure. These modes are shown in Figure 7(a-c) and will be discussed in the following sections. The ratio of (H/B) used in all analyses is equal to 3 in order to guarantee that the "bearing capacity" mode dominates the limit load of the footing-on-slope system. This is further explained in the following section.

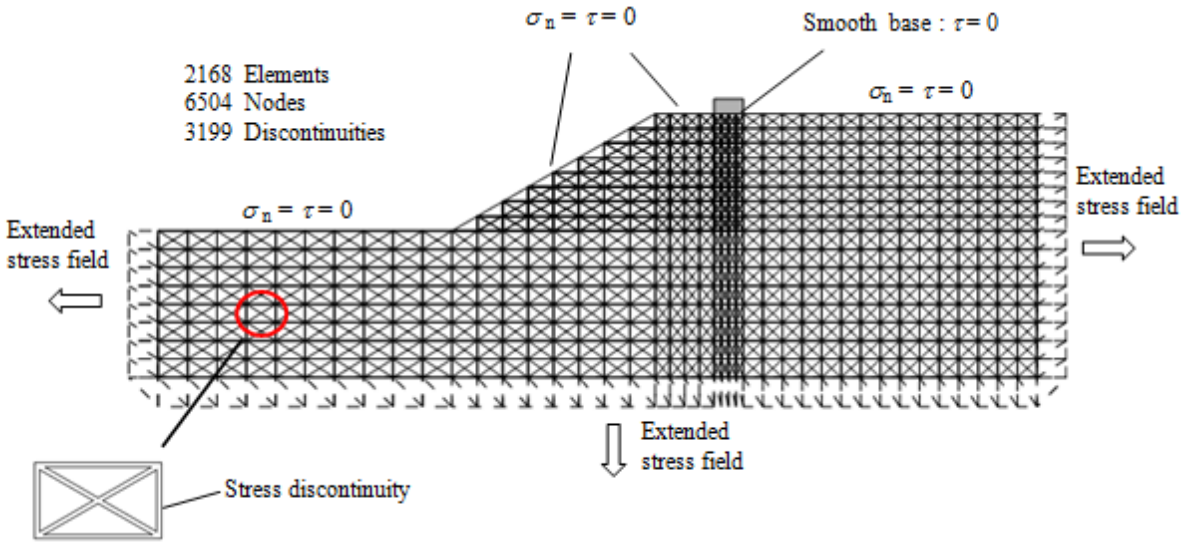

Fig. 6. Typical finite element mesh used in lower bound analysis (β = 30˚, a/B = 2).

Potential Failure Modes for the Footing-on-Slope Problem

Figure 7 shows different typical failure modes for the footing-on-slope problem. Failure mode (a) can be seen when the slope is stable itself and the footing reaches its limit pressure. Failure mode (b) is known as a overall slope failure and occurs under gravitational loading due to the weight of the soil mass. Failure mode (c) happens when the footing distance to the crest of the slope becomes large and the effect of slope angle gets slight and the system resembles to the bearing capacity of a footing on level ground.

Comparison of Results with Some Other Methods

In order to verify the method used in this study, the obtained results are compared with results acquired from other researches. In Figure 8, values of N_c are plotted against various values of ($c/\gamma B$) for an undrained condition (ϕ = 0) with a slope with β =30˚ and (a/B) = 0. These values are obtained according to solutions of Hansen (1961), Vesic (1975), Kusakabe et al. (1981), Narita and Yamaguchi (1990) and Georgiadis (2010). In these analyses, the dimensionless factor of N_c is considered as $N_c = p/c$ where p is the ultimate pressure under footing and c is the cohesion of the soil. For low values of $c/\gamma B$ ($c/\gamma B$ <0.5), the present lower bound solution is not converged and the overall slope failure (failure mode b) occurs. This failure mode can also be observed in the upper bound solution of Kusakabe et al., the finite element solution of Georgiadis and the limit equilibrium solution of Narita & Yamaguchi. For $c/\gamma B \geq 1$ there is a good agreement between the LB solution and other methods; for example, the maximum difference is about -7% with respect to the solution presented by Narita & Yamaguchi for $c/\gamma B$ = 25, while the corresponding values for the N and Y and current LB methods are 4.26 and 3.96, respectively.

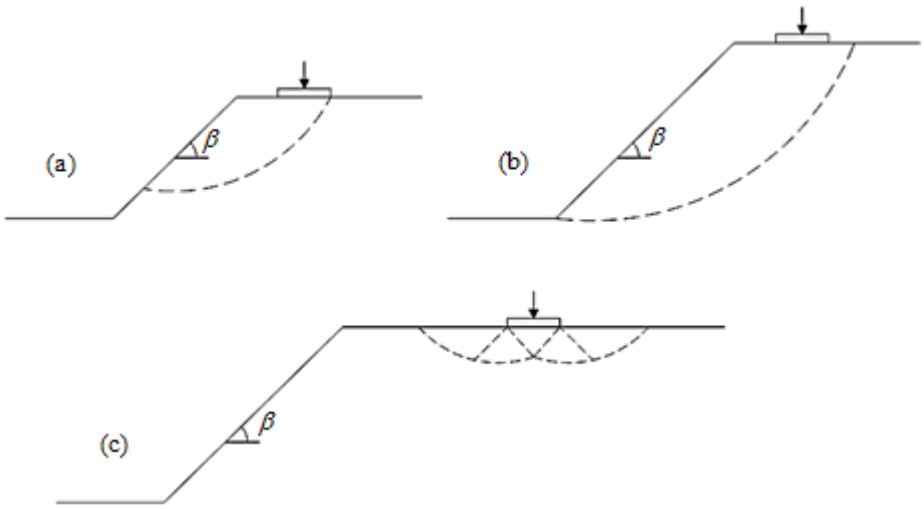

Fig. 7. Different typical failure modes for footing-on-slope problem: bearing capacity failure (a, c) and overall slope failure (b).

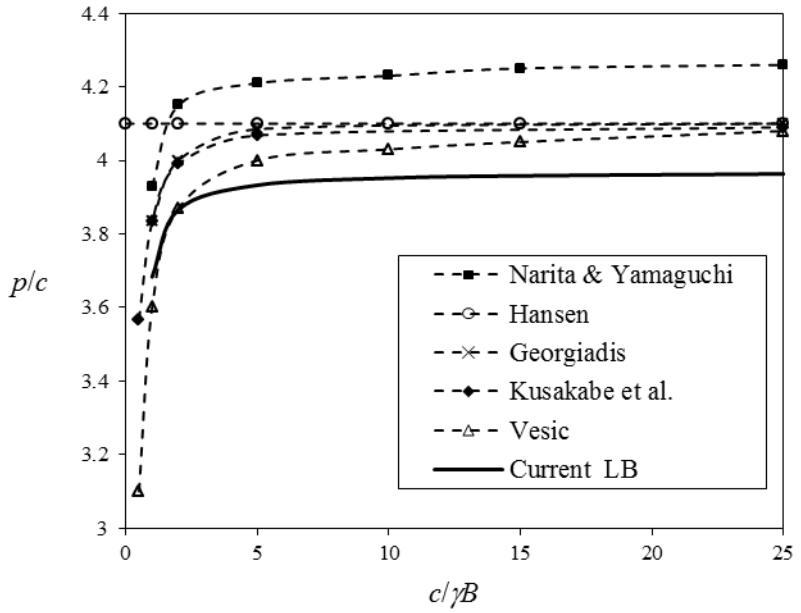

Fig. 8. Variation of bearing capacity with c/γ B (β = 30˚, a/B = 0, ϕ = 0).

Shiau et al. (2011) obtained the undrained bearing capacity of strip footings near slopes using the finite-element limit analysis method and proposed design charts based on averaged LB and UB results. Figure 9 shows a comparison between the current LB solution under β = 60˚ a/B =2, as presented by Shiau et al. and various values of $c/\gamma B$. The maximum difference is about -5.6 % which is related to $c/\gamma B$ =10, while the corresponding value under the method presented by Shiau et al is 48.75 and the current LB method is 46.02.

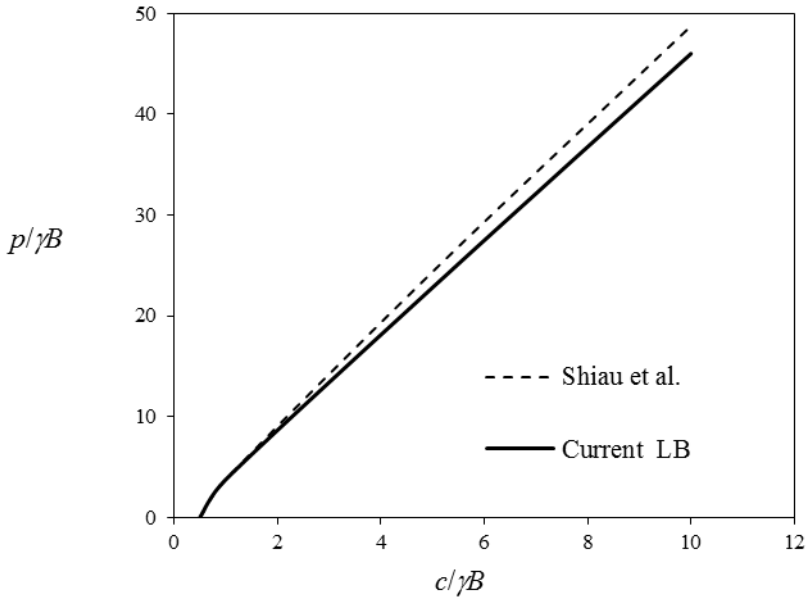

Fig. 9. Variation of bearing capacity with c/γ B (β = 60˚, a/B = 2, ϕ = 0).

RESULTS AND DISCUSSION

As mentioned before, in the current study, the H/B is considered to be 3 in all analyses in order to ensure that the bearing capacity mode of the footing-on-slope system (Failure modes a and c in Figure 7) will occur.

Figure 10 shows the undrained dimensionless limit pressure $p/\gamma B$ for various values of H/B, $c/\gamma B$ ratios of 0.5, 1, 1.5, 2.5, 5 and slopes with $\beta = 30^\circ$ and $\beta = 60^\circ$ while $a/B = 0$. For low ratios of $c/\gamma B$ (i.e. $c/\gamma B \leq 0.5$), the bearing capacity of the footing is negligible and the overall slope failure occurs even for low ratios of H/B. For higher values of $c/\gamma B$ (i.e. $c/\gamma B \geq 1$), charts can be divided into three main parts. The initial part, which takes place at low ratios of H/B (i.e. $H/B \leq 1$), begins with a certain value of $p/\gamma B$ and decreases steeply down to reach a constant value. This part of the diagrams shows a transition from the bearing capacity of a footing rested on level ground to the bearing capacity of a footing rested on a slope. The starting point of this part shows the bearing capacity of a footing on level ground and the ending point shows the bearing capacity of that footing on the slope. The intermediate part of the diagrams is related to failure mode (a) in which the failure mechanism extends to the slope in a way that it is not affected by the height of the slope. In this part, the bearing capacity remains constant until the height of the slope (H/B) reaches a critical value. The third part of the diagrams, which is related to failure mode (b), begins when the slope height approaches its critical value and the overall slope failure happens due to gravity force.

The range of the intermediate part and ultimate slope height increases as the ratio of $c/\gamma B$ increases. As the aim of the present study is to estimate the bearing capacity of footings near slopes, the ratio of H/B should be adopted so that the overall slope failure doesn't occur. So, the H/B ratio is considered to be 4 in all analyses by which failure mode (b) doesn't take place. For a slope with $\beta = 90^\circ$, the results show that using the H/B ratio of 3 is also enough in this case. As the bearing capacity diagrams seen in Figure 10 are generated for an undrained condition and $a/B = 0$, for a drained condition and $a/B \geq 0$ these results are conservative and assuming the H/B ratio equal to 3 is adequate for other cases.

Shiau et al. (2011) proposed a procedure for distinguishing between the bearing capacity failure and overall slope failure which was based on the stability number of slopes. Taylor's stability number (1937) is stated as:

$$N = \frac{c}{\gamma H F_s} \tag{10}$$

where N = stability number, γ = unit weight of the soil, H = height of the slope, F_s = factor of safety for stability of the slope.

Taylor (1937) used the friction circle method (ϕ – circle method) and presented his stability charts based on the friction angle of the soil (ϕ) and the slope angle (β). Michalowski (1995) also presented stability charts using upper bound limit analysis.
Multiplying H/B to Eq. (9) and assuming $F_s = 1$, we obtain (Shiau et al., 2011):

$$N\frac{H}{B} = \frac{c}{\gamma H F_s}\frac{H}{B} = \frac{c}{\gamma B} \tag{11}$$

for Fs =1

or

$$N\frac{H}{B} = \left(\frac{c}{\gamma B}\right)_{crit} \tag{12}$$

for Fs =1

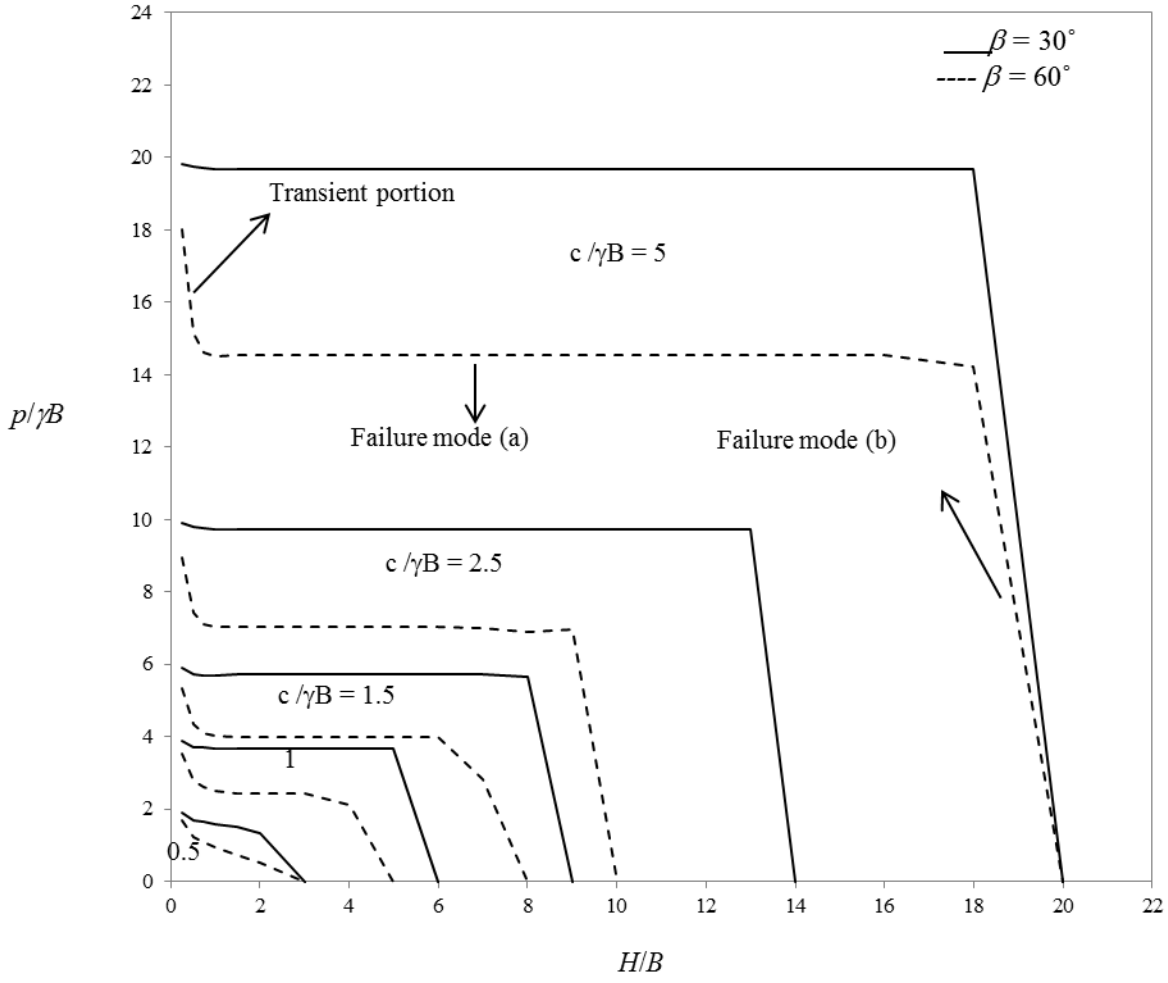

Fig. 10. Effect of H/B on bearing capacity (a/B = 0, ϕ = 0).

To determine the stability of a slope merely (only under gravitational loading), we should follow these steps:

1. Specify the stability number (N) having ϕ and β and using stability charts (Taylor's charts) by assuming F_s =1.
2. Multiply H/B to N and get $(c/\gamma B)_{crit}$ by the use of Eq. (11).
3. Calculate the ratio of $c/\gamma B$ for the footing-on-slope problem.
4. If $c/\gamma B > (c/\gamma B)_{crit}$ then the slope is stable and the bearing capacity failure mode will dominate, but if $c/\gamma B \leq (c/\gamma B)_{crit}$ the overall slope failure mode takes place.

The results of the procedure suggested by Shiau et al. (2011) agree with charts presented in Figure 10. For example, for β = 30˚ and $c/\gamma B$ = 2.5, the critical ratio of H/B is about 13.5 according to Figure 8. Using the stability charts for β = 30˚ and ϕ = 0, the stability number is equal to 0.18. By applying Eq. (11), the critical value of H/B obtained is about 13.9 for $c/\gamma B$ = 2.5 which is close to the diagram result.

The bearing capacity of the footing-on-slope system increases when the footing goes far from the crest of the slope. This is because of the slope angle effect which is diminished and the so-called system approaches to the bearing capacity of a footing on level ground. Such a conclusion cane be derived from Figures 11 and 12 in which the bearing capacity increases as the ratio of a/B goes up. For example, for β = 90˚, $c/\gamma B$ =1 and ϕ = 0 the dimensionless bearing capacity, $p/\gamma B$, increases from 0.99 to 4.46 when the distance of the footing changes from 0 to 10 (Figure 11).

Referring to Figures 11 and12, it can be found out that when the slope angle lessens, the ratio of a/B gets smaller when the bearing capacity remains constant. In other words, the effect of a/B is diminished more rapidly as the slope angle reduces. With reference to Figure 11, for ϕ = 0 and $c/\gamma B$ =1, when the ratio of a/B reaches 2 ($a/B \geq 2$) the bearing capacity of a footing doesn't change for a slope angle of β = 30˚. This ratio is 6 for β = 60˚ and 10 for β = 90˚.

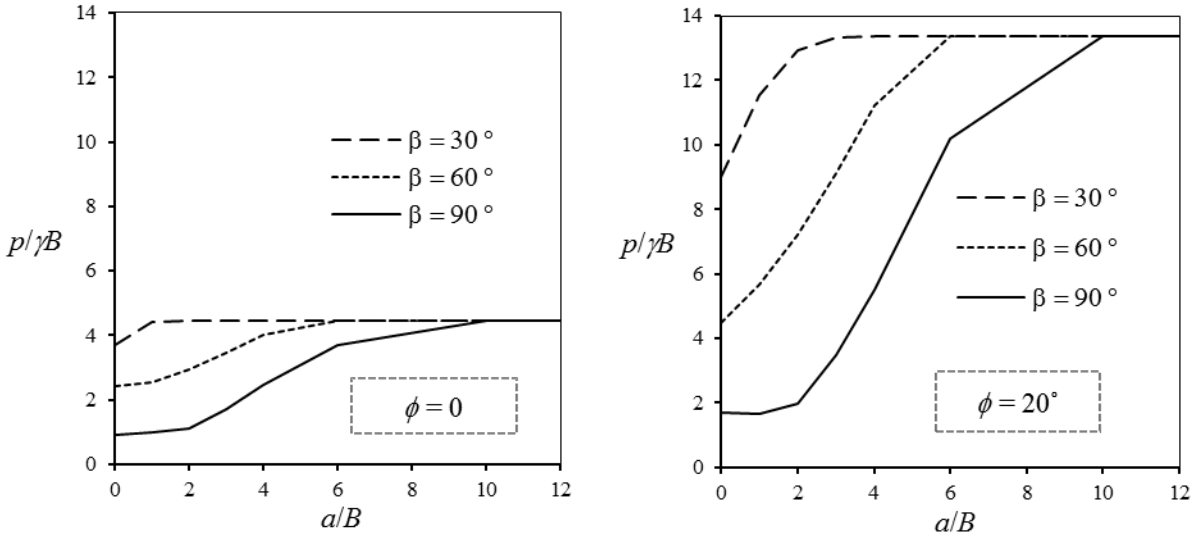

Fig. 11. Effect of a/B and ϕ on bearing capacity ($c/\gamma B = 1$).

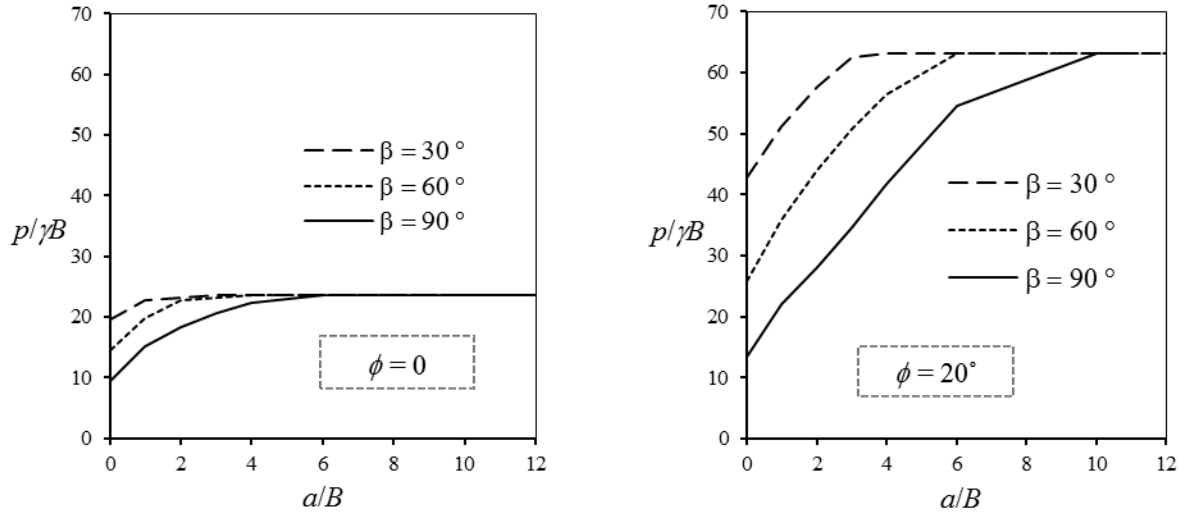

Fig. 12. Effect of a/B and ϕ on bearing capacity ($c/\gamma B = 5$).

The dimensionless strength parameter due to cohesion of the soil ($c/\gamma B$) plays an important role in the stability of footings near slopes. The comparison of Figure 11 and Figure 12 indicates that the bearing capacity increases as the ratio of $c/\gamma B$ increases.

Design charts (Figures 16-20) show that the variation of dimensionless bearing capacity $p/\gamma B$ with $c/\gamma B$ is linear except for low ratios of $c/\gamma B$ ($\leq$0.5). For low values of $c/\gamma B$ ($\leq$0.5), the limit pressure drops to zero and the overall slope failure occurs, as it can be seen in the initial nonlinear dropping part of design charts (Shiau et al., 2011).

The bearing capacity of footings on slopes lessens as the slope angle increases (Figure 13). It should be noted that the effect of the slope angle weakens when the footing gets far from the slope crest and when it reaches a definite distance from the crest; the limit pressure remains constant for all slope angles. This can be observed in Figures. 11, 12 and design charts (Figures 16-20).

The cohesive-frictional soil (drained condition) leads to a notably higher bearing capacity for the footing-on-slope system in comparison with purely cohesive soil (undrained condition). This is due to the effect of the soil friction angle on the stability of such a system by making the failure mechanisms deeper and harder to occur. This can be concluded from Figure 14 where the charts of the bearing capacity of a slope with β = 30˚, $c/\gamma B$= 5 and various values of a/B are generated for $\phi = 0$, $\phi = 10^{\circ}$, $\phi = 20^{\circ}$ and $\phi = 30^{\circ}$. It is seen that the dimensionless limit pressure ($p/\gamma B$) increases by the increase of ϕ. For example, for a/B = 4, the dimensionless bearing capacity rises from 23.45 to 56.98 as the friction angle ϕ increases from 0 to 20˚. The enhancive effect of the soil friction angle can also be deduced by comparing Figures 16-20. Another note is that by an increase of ϕ, the bearing capacity diagrams for various slope angles join together at a higher ratio of a/B.

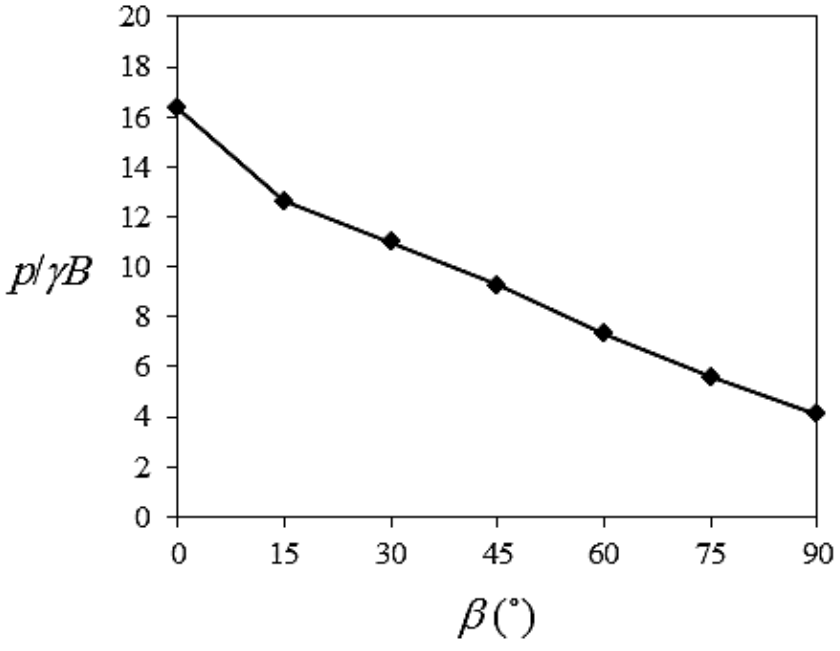

Fig. 13. Variation of bearing capacity with slope angle ($\phi = 10^{\circ}$, $a/B = 0$, $c/\gamma B = 2$).

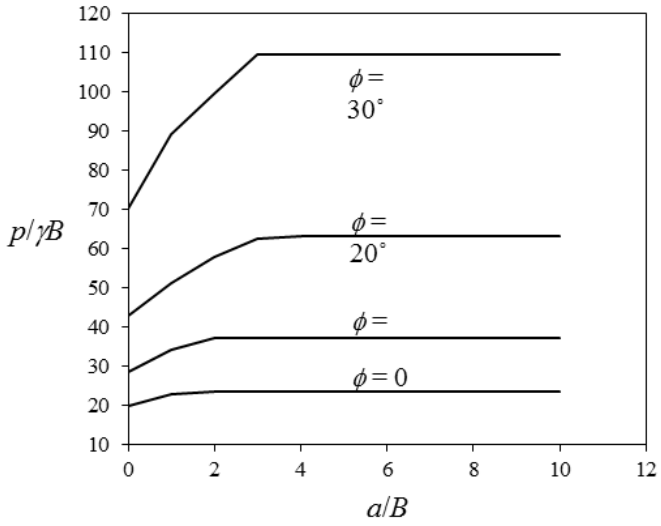

Fig. 14. Effect of ϕ on bearing capacity (β=30˚ , $c/\gamma B = 5$).

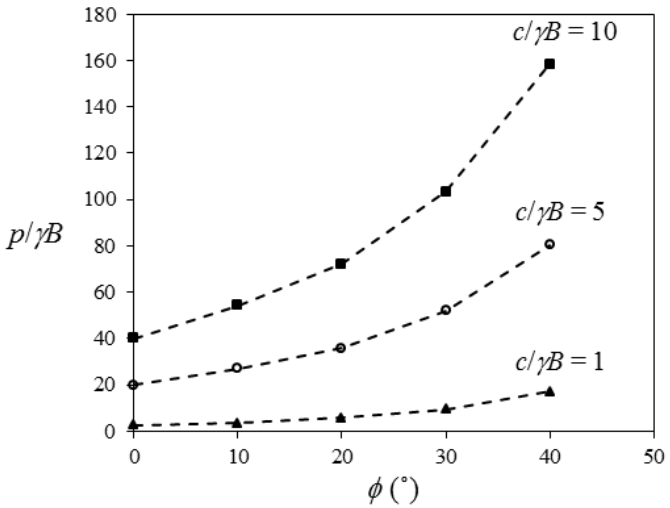

Fig. 15. Variation of bearing capacity with friction angle of the soil (β =60˚, a/B = 1).

Figure 15 also shows the important role of the soil friction angle in improving the bearing capacity of a footing near a slope. It is seen that when the ratio of $c/\gamma B$ increases, the effect of ϕ becomes more significant and the bearing capacity increases more steeply with the increase of ϕ.

Design Charts

In this section, the design charts for lower bound estimation of the bearing capacity of strip footings near slopes are presented. These charts cover various slope angles (β = 30˚, 60˚, 90˚), various footing distances (a/B = 0, 1, 2, 4, 6, 10) and different friction angles of the soil (ϕ=0˚, 10˚, 20˚, 30˚, 40˚). Using the procedure suggested by Shiau et al. (2011) and checking the stability of the slope by calculating $(c/\gamma B)_{crit}$, if the slope is stable Figures 16-20 can be used for determining the bearing capacity of the footing-on-slope problem.

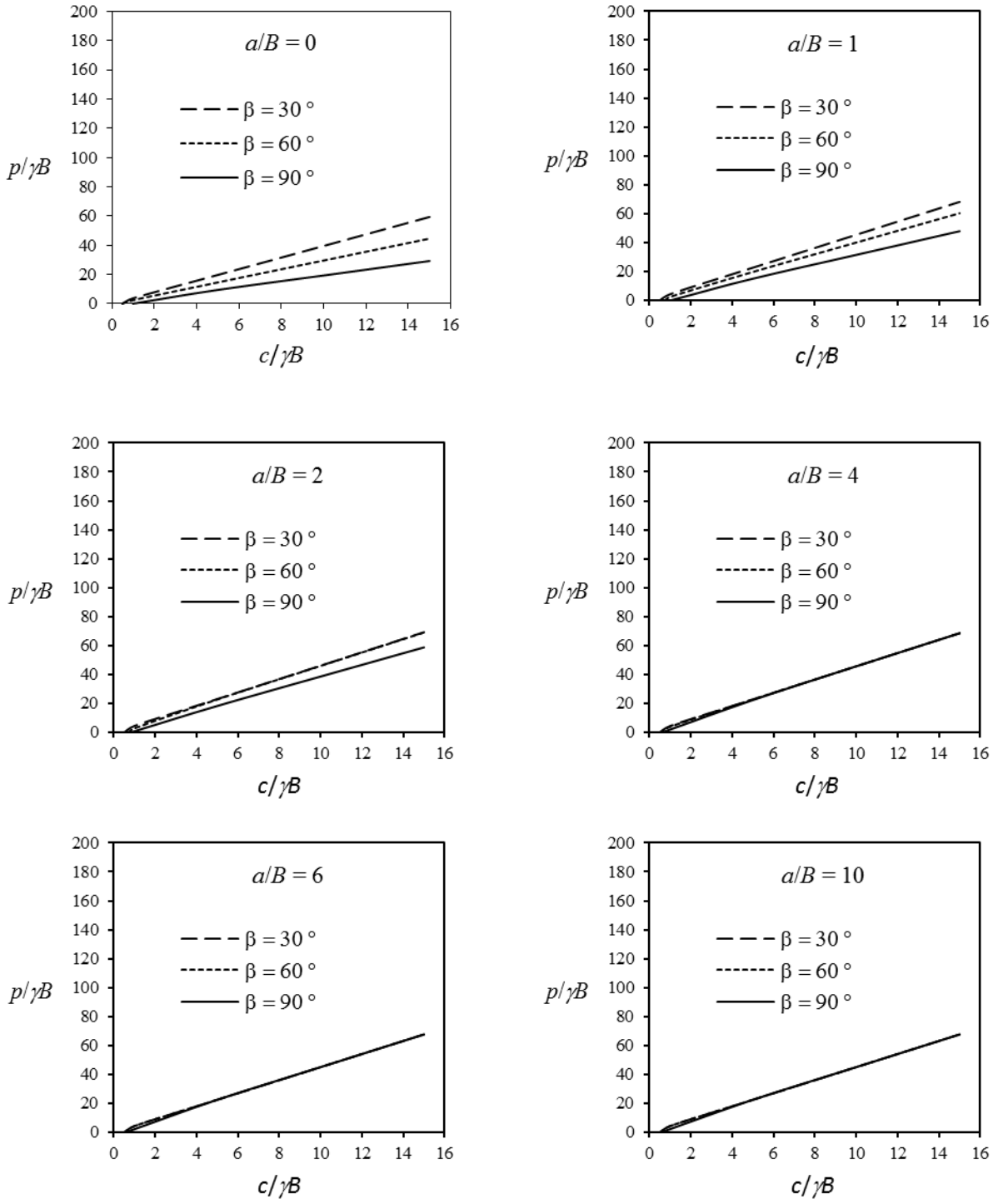

Fig. 16. Bearing capacity charts for various slope angles and footing distances ($\phi = 0$).

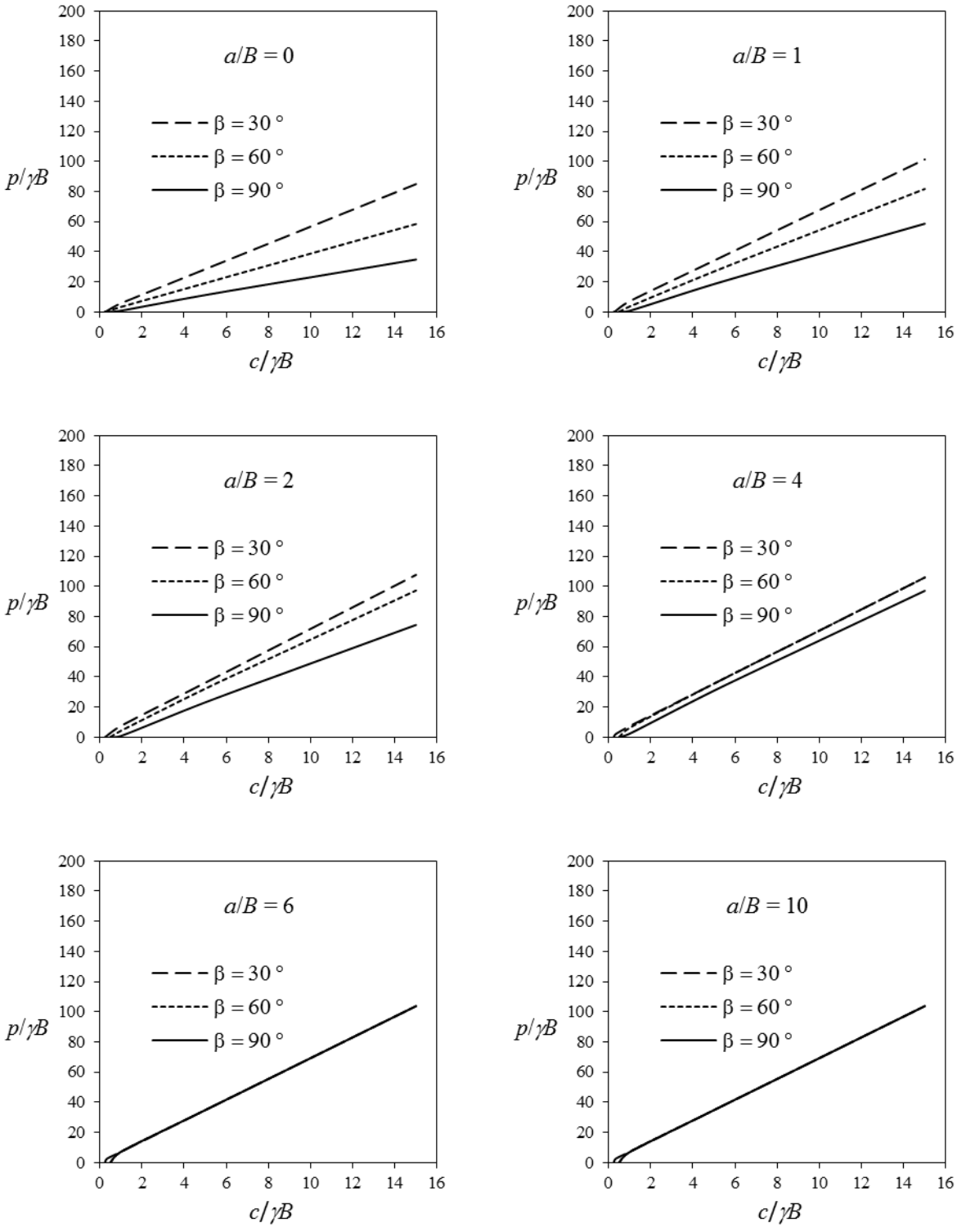

Fig. 17. Bearing capacity charts for various slope angles and footing distances ($\phi = 10^{\circ}$).

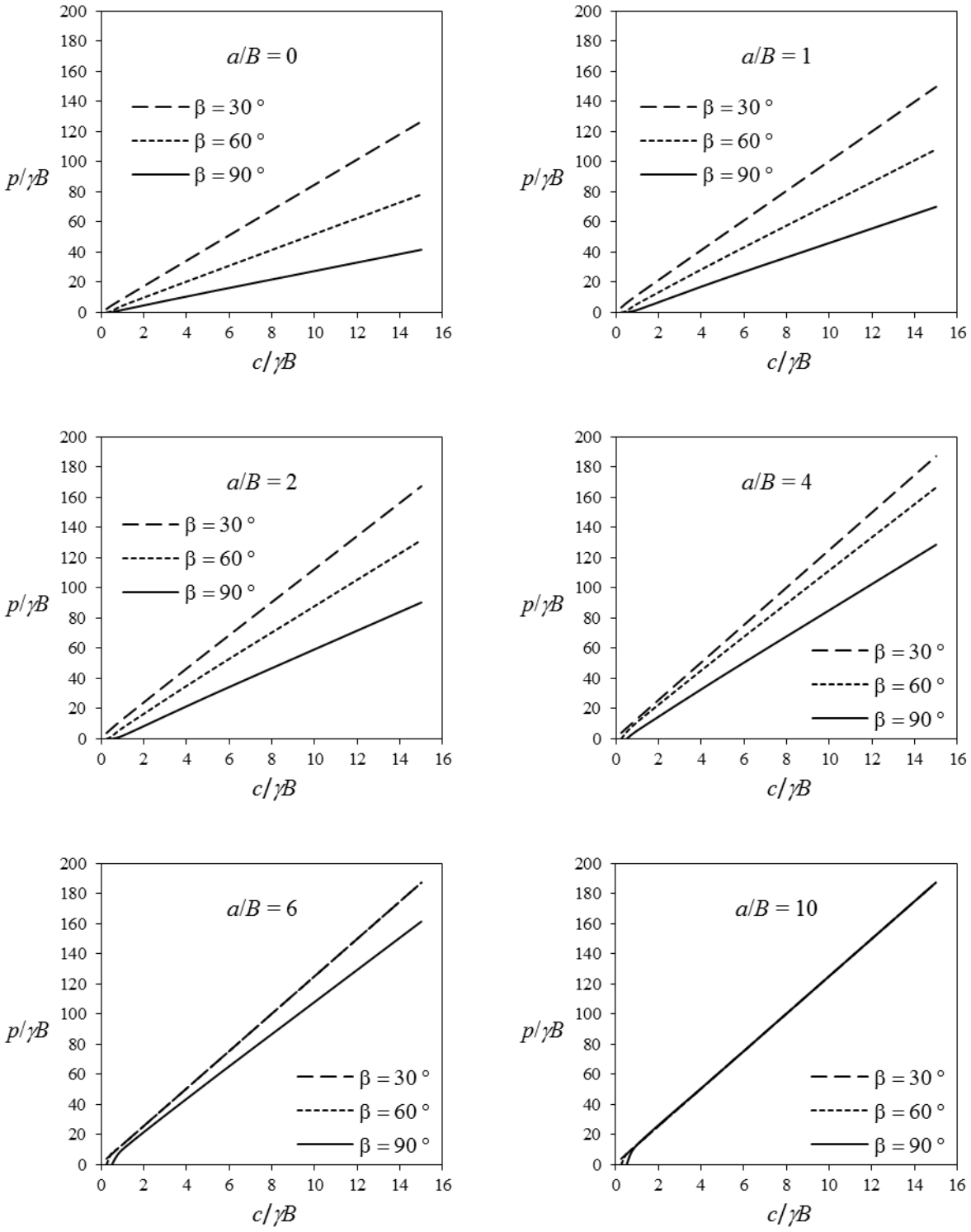

Fig. 18. Bearing capacity charts for various slope angles and footing distances ($\phi = 20^{\circ}$).

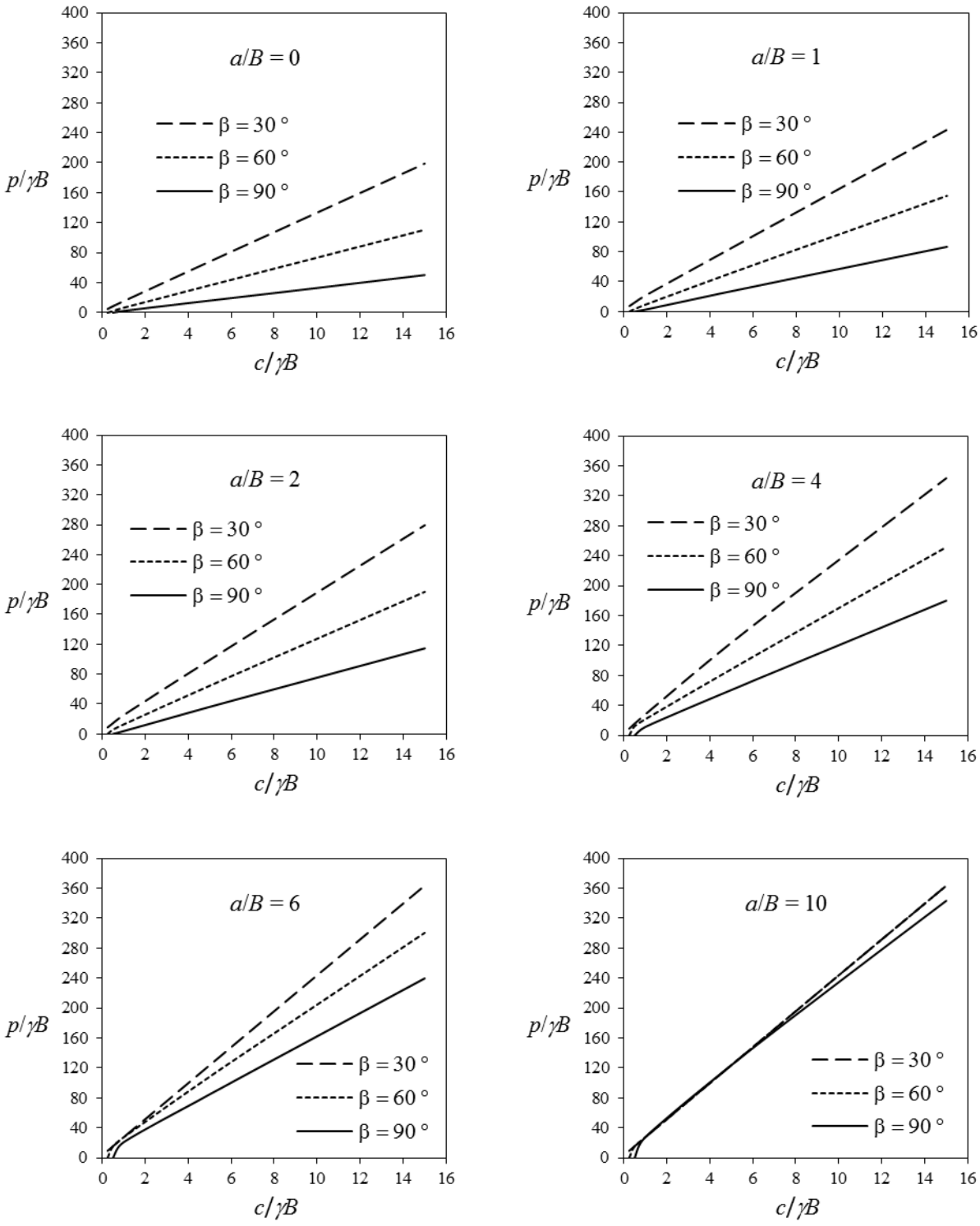

Fig. 19. Bearing capacity charts for various slope angles and footing distances ($\phi = 30^{\circ}$).

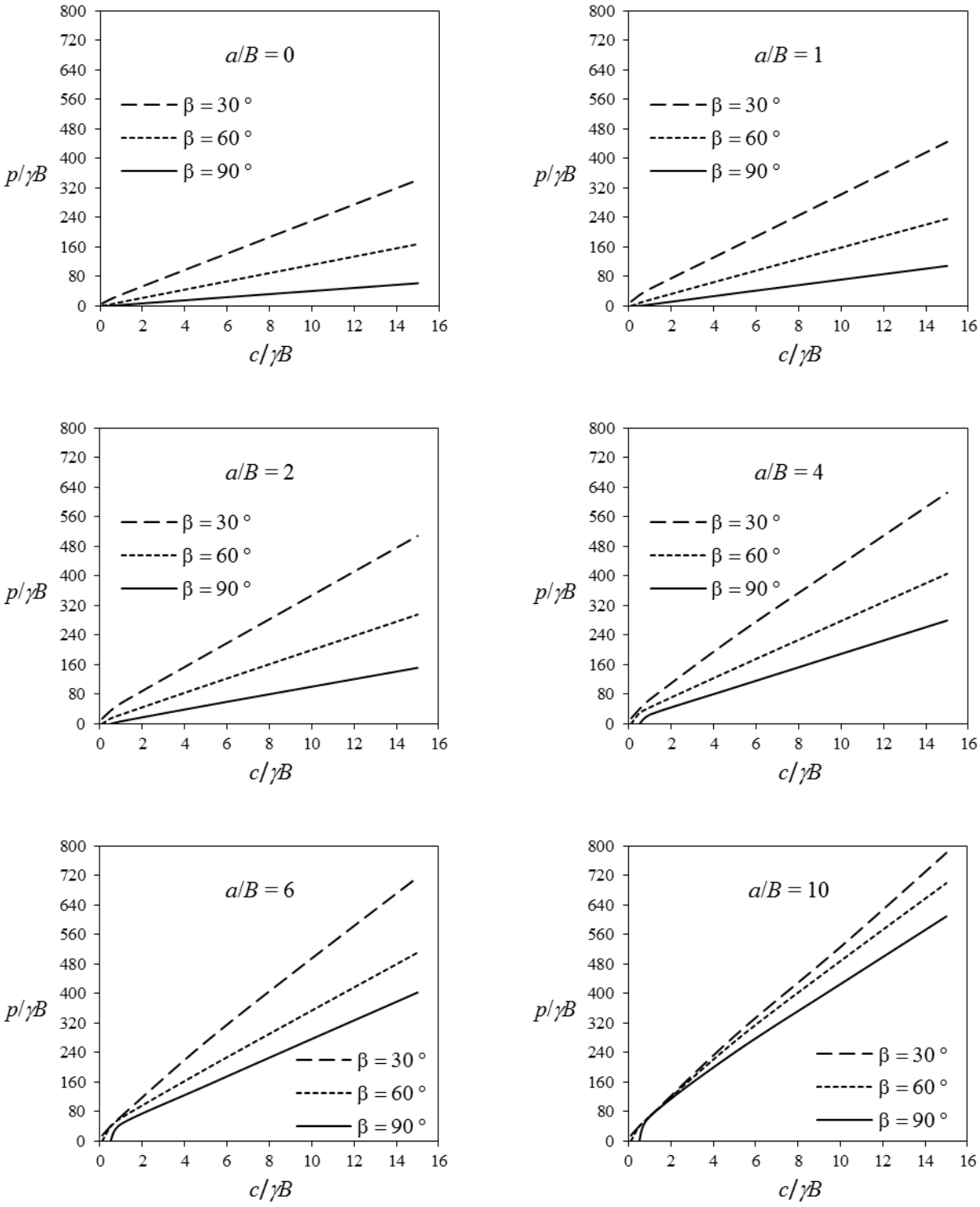

Fig. 20. Bearing capacity charts for various slope angles and footing distances ($\phi = 40^{\circ}$).

EXAMPLE OF APPLICATION

To illustrate the utilization of the design charts presented in the current study, the following problem will be solved.

A smooth strip footing with a width of 1.0 m is to be built 4.0 m far from the crest of a slope with a height of 4.0 m and an angle of 60˚. The soil has the unit weight of γ = 20 kN/m^3, c = 60 kPa and ϕ = 20˚. In this problem, the ultimate bearing capacity of the footing should be determined.

1. For a slope with β = 60˚ and ϕ = 20˚, using Taylor's stability charts, a value of 0.095 is obtained for N.
2. Using Eq. (11), we have $(\frac{c}{\gamma B})_{crit} = N\frac{H}{B} = 0.095(\frac{4}{1}) = 0.38$
3. $\frac{c}{\gamma B} = \frac{60}{20(1)} = 3$
4. $\frac{c}{\gamma B} > (\frac{c}{\gamma B})_{crit}$, therefore the slope is stable and we can use the design charts for lower bound estimation of the bearing capacity.
5. With ϕ = 20˚, we use Figure 18 for $\frac{c}{\gamma B} = 3$, a/B = 4 and β = 60˚ which leads to the dimensionless bearing capacity of $\frac{p}{\gamma B} \approx 32$. Thus, the ultimate load is $P = 32(20)(1) = 640$ kPa.

CONCLUSIONS

The bearing capacity of strip footings adjacent to slopes is investigated using the finite element-lower bound method. The normalized bearing capacity is considered as the ratio of ($p/\gamma B$) where p is the average limit pressure under the footing base. The effect of various parameters on the bearing capacity of a footing-on-slope system are studied. It is seen that the friction angle of the soil (ϕ) has a great effect on the bearing capacity of the so-called system. The combination of two dominant failure modes (overall slope failure mode and bearing capacity failure mode) makes the footing-on-slope problem complex. It is observed that for low values of $c/\gamma B$ the global slope failure occurs. Moreover, for a definite value of $c/\gamma B$, there is a critical ratio of H/B by which the global slope failure occurs and the slope becomes unstable merely under gravitational loading. The stability of the mere slope (without footing) can be distinguished by the procedure suggested by Shiau et al. (2011). When the slope is stable itself, then the linear part of the design charts (Figures 16-20) can be used for lower bound estimation of the bearing capacity of strip footings on slopes.

REFERENCES

Azzouz, A.S. and Baligh, M.M. (1983). "Loaded areas on cohesive slopes", *Journal of Geotechnical Engineering*, 109(5), 724–729.

Castelli, F. and Motta, E. (2008). "Bearing capacity of shallow foundations near slopes: Static analysis", *Proceedings of the Second International British Geotechnical Association Conference on Foundations, ICOF 2008*, HIS BRE Press, Watford, U.K., 1651–1660.

Davis, E.H. and Booker, J.R. (1973). "Some adaptations of classical plasticity theory for soil stability problems", *Proceedings of the Symposium on the Role of Plasticity in Soil Mechanics*, A.C. Palmer, ed., Cambridge University, Cambridge, UK, 24–41.

de Buhan, P. and Garnier, D. (1994). "Analysis of the bearing capacity reduction of a foundation near a slope by means of the yield design theory", *Revue Française de Géotechnique*, 68, 21–32. (in French).

de Buhan, P. and Garnier, D. (1998). "Three dimensional bearing capacity of a foundation near a slope", *Soils Foundation*, 38(3), 153–163.

Drucker, D.C., Greenberg, W. and Prager, W. (1952). "Extended limit design theorems for continuous media", *Quarterly of Applied Mathematics*, 9, 381–389.

Farzaneh, O., Askari, F. and Ganjian, N. (2008). "Three dimensional stability analysis of convex slopes in plan view", *ASCE, Journal of Geotechnical and Geoenvironmental Engineering*, 134(8), 1192-1200.

Georgiadis, K. (2010). "Undrained bearing capacity of strip footings on slopes", *ASCE, International journal of Geotechnical and Geoenvironmental Engineering*, 136(5), 677-685.

Hansen, J.B. (1961). "A general formula for bearing capacity", *Bulletin 11, Danish Geotechnical Institute*, Copenhagen, Denmark, 38–46.

Krabbenhoft, K., Lyamin, A.V., Hjiaj, M. and Sloan, S.W. (2005). "A new discontinuous upper bound limit analysis formulation", *International Journal for Numerical Methods in Engineering*, 63(7), 1069–1088.

Kusakabe, O., Kimura, T. and Yamaguchi, H. (1981). "Bearing capacity of slopes under strip loads on the top surface", *Soils Foundation*, 21(4), 29–40.

Lyamin, A.V. (1999). "Three-dimensional lower bound limit analysis using nonlinear programming", Ph.D. Thesis, University of Newcastle, Australia.

Lyamin, A.V. and Sloan, S.W. (2002a). "Lower bound limit analysis using non-linear programming", *International Journal for Numerical Methods in Engineering*, 55(5), 573–611.

Lyamin, A.V. and Sloan, S.W. (2002b). "Upper bound limit analysis using linear finite elements and non-linear programming", *International Journal for Numerical and Analytical Methods in Geomechanics*, 26(2), 181–216.

Lyamin, A.V., and Sloan, S.W. (2003). "Mesh generation for lower bound limit analysis", *Elsevier Science, International Journal for Advances in Engineering Software*, 34(6), 321–338.

Lysmer, J. (1970). "Limit analysis of plane problems in soil mechanics", *J. Soil Mechanics Foundation Division, ASCE*, 96 (SM4), 1311-1334.

Meyerhof, G.G. (1957). "The ultimate bearing capacity of foundations on slopes", *The Proceedings of the Fourth International Conference on Soil Mechanics and Foundation Engineering*, London, 384–386.

Michalowski, R.L. (1989). "Three-dimensional analysis of locally loaded slopes", *Géotechnique*, 39(1), 27–38.

Michalowski, R.L. (1995). "Slope stability analysis: a kinematical approach", *Geotechnique*, 45(2), 283–293.

Narita, K. and Yamaguchi, H. (1990). "Bearing capacity analysis of foundations on slopes by use of log-spiral sliding surfaces", *Soils Foundation*, 30(3), 144–152.

Shiau, J.S., Lyamin, A.V. and Sloan, S.W. (2003). "Bearing capacity of a sand layer on clay by finite element limit analysis", *Canadian Geotechnical Journal*, 40(5), 900–915.

Shiau, J.S., Merifield, R.S., Lyamin, A.V. and Sloan, S.W. (2011). "Undrained stability of footings on slopes", *ASCE, International Journal of Geomechanics*, 11(5), 381-390.

Sloan, S.W. (1988). "Lower bound limit analysis using finite elements and linear programming", *International Journal for Numerical and Analytical Methods in Geomechanics*, 12(1), 61–67.

Sloan, S.W. (1989). "Upper bound limit analysis using finite elements and linear programming", *International Journal of Numerical and Analytical Methods in Geomechanics*, 13(3), 263–282.

Sloan, S.W. and Kleeman, P.W. (1995). "Upper bound limit analysis using discontinuous velocity fields", *Computer Methods in Applied Mechanics and Engineering*, 127(1-4), 293–314.

Sokolovski, V.V. (1960). *Statics of granular media*, Butterworth Scientific Publications, London.

Taylor, D.W. (1937). "Stability of earth slopes", *Journal of the Boston Society of Civil Engineers*, 24(3), 197–247.

Vesic, A.S. (1975). *Bearing capacity of shallow foundation*, Foundation engineering handbook, H.F. Winterkorn, and H.Y. Fang, (eds.), Van Nostrand Reinhold, New York.